Spin stiffness of a Fermi liquid in the $\nu = 1$ quantum Hall regime

A. B. Van'kov and I. V. Kukushkin
Institute of Solid State Physics, RAS, Chernogolovka 142432, Russia
and Laboratory for Condensed Matter Physics, National Research University Higher School of Economics, Moscow 101000, Russia

(Received 27 August 2020; revised 23 November 2020; accepted 7 December 2020; published 21 December 2020)

Anomalous behavior of spin stiffness is revealed in ZnO-based two-dimensional electron systems (2DESs) with strong Coulomb interaction and Wigner-Seitz parameter $r_s > 6$. The spin stiffness is extracted directly from the quadratic k dispersion of spin excitons at $\nu = 1$ probed by inelastic light scattering. The resulting values are found to be dramatically rescaled compared to the case of weakly interacting 2DESs—spin stiffness turned out to be of the order of the cyclotron energy with the effective mass of Fermi-liquid quasiparticles. This result is also confirmed by the exact diagonalization simulations.

DOI: 10.1103/PhysRevB.102.235424

I. INTRODUCTION

The behavior of two-dimensional electron systems (2DESs) with a strong Coulomb interaction sometimes breaks down well-established models for their description. Thus, the physics of the quantum Hall effect, full of spectacular events and facts, has acquired a new stream of puzzles with the advent of new ultrapure strongly interacting 2DESs based on MgZnO/ZnO heterostructures [1]. The parametric space of such electron systems is radically different from the widely exploited GaAs/AlGaAs platform in terms of comparatively stronger Coulomb interaction, a fivefold decrease in kinetic energy, and an equally significant increase in Zeeman splitting. In addition to the appearance of new exotic phases of the fractional quantum Hall effect [2], states with integer filling factors also undergo qualitative transformations: the paramagnetic state with $\nu = 2$ undergoes ferromagnetic instability, having a purely many-particle origin [3]. Similar events occur with other even- and odd-integer filling factors [2,4]. Surprisingly, the most stable quantum Hall ferromagnetic state $\nu = 1$ did not remain unchanged—the enhanced Coulomb interaction has led to the opposite effect on the scale of the exchange energy at the lowest Landau level (LL) [5]. All these facts cannot be explained even qualitatively in terms of single-particle electron states in the hierarchy of LLs—their mixing is too significant. Alternatively, the electron recombination spectra from LLs indicate that the state of strongly interacting 2D systems is better described in the concept of Fermi-liquid quasiparticles, surviving not only near the surface of the Fermi sea but also in its depths [6,7]. This equally refers to the Hall quantization of quasiparticles. The microscopic mechanism of such a renormalization is still unknown. Nevertheless, it is sometimes very helpful to consider many-particle problems independently in terms of individual electrons and in terms of Fermi-liquid quasiparticles and to catch similarities and differences. In the context of studying the many-particle interaction effects in quantum Hall systems, the method of sensing the simplest collective excitations is especially effective. The energy structure of such neutral excitations, referred to as *magnetoexcitons* [8], depending on their type, can include terms related to the cyclotron gap (upon the transition of electrons between different LLs), the one-particle Zeeman splitting parameter (for spin-flip process), and the many-particle contribution, determining the magnetoexciton dispersion. In the long-wavelength limit, the motion of magnetoexcitons is least affected by residual disorder in the system, and the many-particle contribution to their energy reflects pure correlation and/or exchange corrections. This is what makes it possible to effectively use the experimental method of inelastic light scattering (or Raman scattering) for direct probing of the many-particle contributions to the energy of collective excitations.

The simplest type of magnetoexcitons at the LLs is the intralevel spin exciton (SE). Its energy at $k = 0$ coincides with the single-particle Zeeman energy, regardless of the value of Coulomb correlations [9] (the so-called Larmor theorem), and in the short-wavelength limit, the main contribution to its energy is determined by the exchange energy of electrons at the occupied LLs. It is not possible to directly measure this exchange contribution to the energy of SEs due to the strong influence of disorder on the energy of collective excitations at large momenta and also due to the influence of spin-texture excitations [10,11].

However, the same value of the exchange energy determines the spin stiffness of the system, which is the ascent of the quadratic dispersion of SE at small momenta. The dispersion can be measured directly by Raman scattering with a variable momentum transfer. The spin stiffness for 2DES at filling $\nu = 1$ with small values of the interaction parameter $r_s \ll 1$ is given by the exchange energy of electrons at the lowest LL $\Sigma \sim \sqrt{\pi/2}e^2/\varepsilon l_B$, where l_B is the magnetic length. Here the Hartree-Fock approximation (HFA) [8,12] perfectly explains the experiment in GaAs structures [13]. In the case of 2DESs with strong Coulomb interaction $r_s \gg 1$, even the structure of the ground state $\nu = 1$ is unknown due to the

mixing of the LLs. However, the SE is still the lowest-energy collective excitation with the Zeeman gap. The spin stiffness for this case was previously estimated in the spirit of Landau's Fermi-liquid theory, and surprisingly, it drops to a value of the order of cyclotron energy [14]. So far, this effect has not been observed experimentally due to its subtlety for heavy-fermion systems and the existing limitations on experimental accuracy.

In this work, the attenuated dispersion of SEs in the ferromagnetic state $\nu = 1$ was explicitly measured by the Raman scattering with high-precision resolution. The spin stiffness parameter was studied on a set of MgZnO/ZnO heterostructures that differ in the parameter of electron density, corresponding to $r_s > 6$. It was found that at $\nu = 1$, the measured spin stiffness is drastically reduced compared to the Coulomb energy scale. The quantitative answer suggests that the softened value is not just of the order of single-particle cyclotron energy; it is determined by the effective mass of the Fermi-liquid quasiparticles. This stiffness serves as a measure of the pure exchange energy in the quantum Hall ferromagnet with strongly interacting electrons. The experimental findings are supported by the calculations using the exact diagonalization for a small number of electrons and independently, in terms of the Fermi-liquid model.

II. EXPERIMENTAL TECHNIQUE

Experimental studies were performed on four MgZnO/ZnO heterostructures grown by molecular beam epitaxy [1]. A 2DES is formed in the ZnO layer near the heterointerface, occupying one size-quantized subband. Electron densities in samples ranged from 1.75×10^{11} to 3.5×10^{11} cm^{-2}, and low-temperature mobilities exceeded 400 000 cm^2/V s. The single-particle 2DES parameters, which are essential for further consideration, were taken from other experimental studies [15,16] and were the following: Landé factor $g^* = 1.95$, cyclotron mass $m_c = 0.3m_0$, and dielectric constant $\varepsilon_{ZnO} = 8.5$. The measurements were carried out in a ^{3}He vapor evacuation cryostat with a bath temperature $T = 0.35$ K in magnetic fields up to 15 T. Optical experiments were performed using a tunable Ti:sapphire laser doubled in frequency with a wavelength in the range of 366–367 nm near the direct optical ZnO gap. In this case, the magnetic field evolution of the photoluminescence signal from 2D electrons was studied in order to determine the magnetic field values corresponding to integer filling factors. The dispersion of collective excitations was measured by the resonant Raman scattering with a tunable transferred momentum and unpolarized configuration. The scattering geometry is illustrated in the inset in Fig. 1(b). Two quartz multimode optical fibers were used for the optical access to the sample: one for photoexcitation and the other for signal collection. The fibers were mounted on a rotational stage, enabling us to change their orientation to the sample surface. The transferred momentum was set by the difference between the projections of the incident and scattered photon momenta to the 2D plane and reached values in the range 0.4×10^5 to 3.3×10^5 cm^{-1}. The numerical aperture (NA) of the optical fibers used in the experiment was NA = 0.11, which led to an

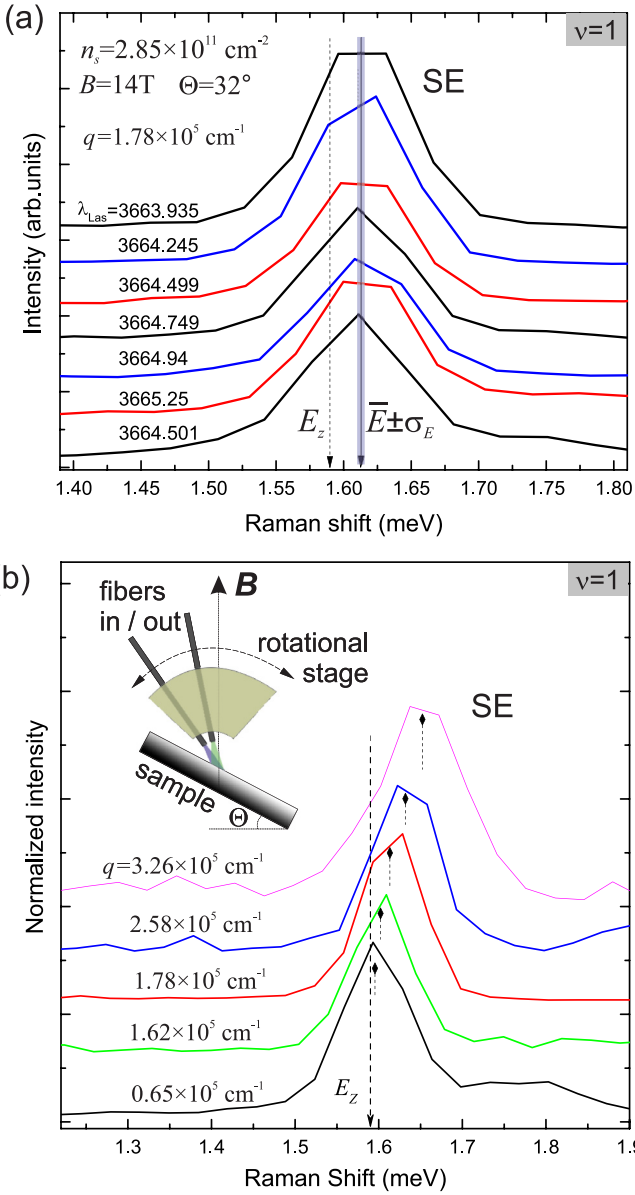

FIG. 1. (a) The cascade of spin exciton Raman spectra at $\nu = 1$, taken at different values of laser wavelengths. The gray bar depicts the extracted average peak position and its standard deviation. The Zeeman energy position is shown by a dashed line. (b) The SE spectra at different values of the 2D momentum. The flags are set on the determined peak positions. The inset illustrates the scattering geometry and the rotational stage for tuning the 2D momentum.

easily calculated uncertainty of the transferred momentum. Optical spectra were detected using a single spectrometer (Monospec) in combination with a CCD camera providing a spectral resolution of 0.05 meV.

To achieve higher momenta in the plane, some samples were also tilted with respect to the magnetic field. Here the influence of the parallel component of the magnetic field on the character of collective excitations was considered insignificant since the corresponding cyclotron energy is two orders of magnitude lower than the intersubband splitting in ZnO heterostructures [17].

III. SPIN STIFFNESS OF A QUANTUM HALL FERROMAGNET AT $\nu = 1$

Figure 1 shows the Raman spectra of the spin exciton at $\nu = 1$ on the heterostructure with electron density $n_s = 2.85 \times 10^{11}$ cm^{-2}. The identification of the spin exciton in the Raman spectra does not present a problem since this collective excitation has an energy close to single-particle Zeeman splitting and also has a natural spectral width orders of magnitude lower than the above-mentioned hardware resolution. Therefore, in all the studied spectral data, the linewidth was equal to the spectrometer resolution. For further refinement of the detected SE energies, we used the method of statistical averaging of the extracted Raman shifts over a sequence of $N \sim 20$–30 spectra measured at different laser wavelengths with other experimental conditions being equal [see Fig. 1(a)]. In such a way, the average peak position $\overline{E}$ and the standard deviation σ_E were extracted [both are shown as a gray bar in Fig. 1(a)]. The latter determined the error in determining the peak position and reached 3–4 μeV.

The Raman shift of the SE peak really evolves as a function of transferred 2D momentum k. This can be seen in the sequence of spectra in Fig. 1(b), where the values of momenta are indicated on spectral curves. The SE dispersion at $\nu = 1$ for this sample is explicitly plotted in Fig. 2(a). To extract the spin stiffness parameter from the dispersion data of SEs, one should represent the long-wavelength fragment of the dispersion in the form $E_{\mathrm{SE}} = E_z + J/2\,(ql_B)^2$, where J is the spin stiffness, l_B is the magnetic length, and ql_B is the dimensionless wave vector. The experimental data in Fig. 2(a) are compared with the analytical dispersion, obtained within the HFA for $\nu = 1$ (neglecting LL mixing). There spin stiffness is $J_{\mathrm{HFA}} = \sqrt{\pi/8}e^2/\varepsilon l_B$, and the corresponding curve is shown by the dashed line. The discrepancy is huge and needs to be further analyzed on other samples. The SE-dispersion data are obtained for all experimental samples, and the k-dependent many-particle contributions are analyzed in Fig. 2(b). For the convenience of comparing the variable part of the dispersion dependence, the terms of the single-particle Zeeman energy were subtracted. The best way to extract the spin stiffness parameter J is to replot the k-dependent energy term using $(ql_B)^2$ as the abscissa and fit it by the least-squares method [Fig. 2(b)]. The resulting values of J are given as a function of electron density in Fig. 3(b) (solid rhombs). The obtained values are incommensurably lower than the calculated values in the HFA model (the steep dotted curve on the graph). This inconsistency clearly demonstrates the fact of strong rescaling of the exchange energy due to LL mixing and the need for the principally different theoretical approach for its proper consideration. The dashed line shows the qualitatively different analytical prediction for spin stiffness at $\nu = 1$; it is the value of the cyclotron energy, as estimated for the case $r_s \gg 1$ using the diagrammatic technique in Ref. [14]. It can be seen from the plot that the experimental stiffness grows in a close-to-linear manner and is, indeed, about $\hbar\omega_c$ and is even smaller.

To describe the softened dispersion of SE, the formalism of the perturbation theory in the parameter r_s is not suitable because for the case $r_s \gg 1$ the influence of LL mixing is great. Electron-electron correlations lead to a redistribution

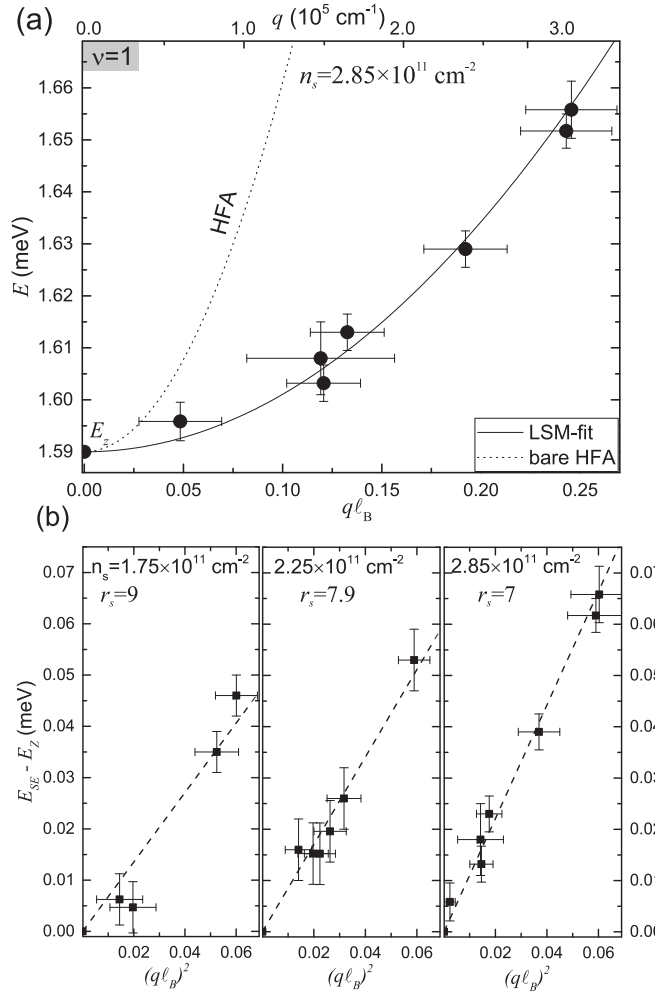

FIG. 2. (a) Plot of the SE k dispersion in the sample with $n_s = 2.85 \times 10^{11}$ cm^{-2}. The fitting line is calculated by the least-squares method; the dotted line is calculated within the HFA and is given for comparison. The lower axis is given in dimensionless units of the wave vector. (b) The SE dispersions in three samples are replotted using $(ql_B)^2$ as the abscissa. The data points fall on a line, where the slope yields an accurate value of the spin stiffness.

of the filling of the LLs, and not only the excited state but also the ground state is unclear. The main starting points in calculating the energy spectrum are the quantum numbers of the system: the total spin and the total momentum. The distribution of electrons in the eigenstates of the system should be taken into account self-consistently under the action of the full Hamiltonian of interacting electrons. This procedure was carried out here by the method of exact diagonalization [18] of the electron spectrum on a finite number of electrons. We took the single-particle band parameters m^* and g^*, the permittivity ε, the total electron density, and the filling factor. The effect of nonlocality of the electron wave function in the lowest-dimensional quantization subband on the Coulomb interaction was also taken into account via the geometric form factor. The latter was done by means of a self-consistent solution of the Schrodinger and Poisson equations at a given electron density. The exact diagonalization calculations were carried out in the geometry of a torus with a rectangular magnetic

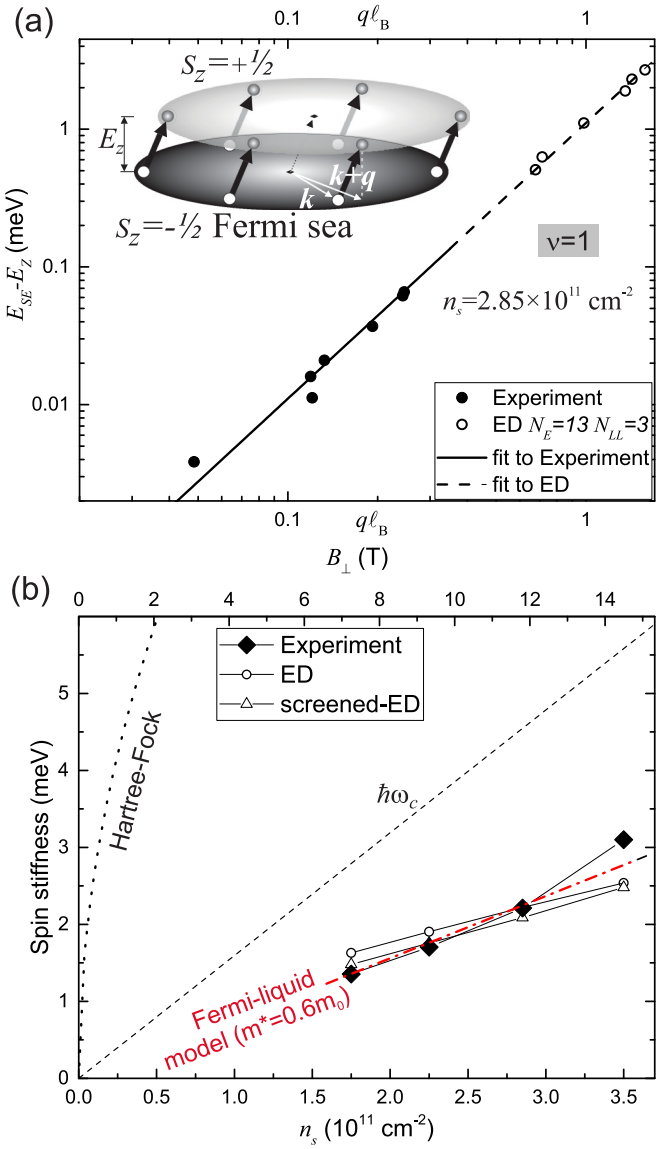

FIG. 3. (a) Joint plot of the SE dispersion at $\nu = 1$ with experimental data (solid circles) and exact diagonalization simulation (open circles). The inset illustrates the SE formation scheme in the representation of Fermi-liquid quasiparticles at weak magnetic field. (b) Spin stiffness parameter as a function of the electron density. The upper axis is given in units of magnetic fields, required for $\nu = 1$. The experimental data (solid rhombs) are compared to the results of the exact diagonalization (open circles), screened ED (open triangles), Hartree-Fock values (dotted curve), cyclotron energy (dashed line), and the Fermi-liquid model, described in the main text (dash-dotted line).

Bravais lattice, with a ratio of linear dimensions in the x-y directions close to unity. For diagonalization at $\nu = 1$, the states of $N_e = 10$–13 distributed over $N_{LL} = 3$ of the lowest LLs were taken into account. Such a large number of LLs taken into account is unusual for the exact diagonalization of the quantum Hall problems. This was done here due to the significant role played by virtual electron transitions between the LLs. The convergence of the numerical answers was checked by varying the parameters of N_e from 10 to 13. In general, the combinatorial capacity of the Hilbert space of many-electron states at such a number of LLs is very large; therefore, to implement the calculations, the basis trimming approach [19] was used, taking the finiteness of the mixing parameter r_s into account.

The results of calculating the SE dispersion for the parameters relevant for the sample with $n_s = 2.85 \times 10^{11}$ cm^{-2} are superimposed on the corresponding experimental data in Fig. 3(a), where the best-fit curves are also shown by solid (experimental) and dashed (calculated) lines. Obviously, the effect of the dispersion softening is achieved qualitatively and even quantitatively. Similar calculations performed for the parameters of all other samples made it possible to extract the dependence of the calculated spin stiffness on the electron density [open symbols in Fig. 3(b)] and compare it with the experimental data (solid rhombs). For such large values of the mixing parameter as $r_s \sim 7$–9, even taking into account the $N = 3$ LLs is not entirely sufficient for the quantitative calculation of many-particle effects. The virtual transitions of electrons to even higher LLs can be taken into account by reducing the Coulomb potential with the static dielectric function $V(q) = 2\pi e^2/\varepsilon\, q\, \epsilon(q)$. This approach, referred to as the *static screening approximation* [20,21], was successfully exploited for simulations in a number of quantum Hall problems for strongly interacting systems, including graphene [22] and ZnO [5,23,24]. The calculations performed for the screened potential with the dielectric function $\epsilon(q)$ taken in the random-phase approximation are shown by open triangles in Fig. 3(b) and are only ~10% weakened relative to the data with the bare Coulomb potential. It should also be taken into account that discrete simulations for a small number of electrons suffer from the coarsening of the calculated energies. In particular, for $N_e = 13$, the underestimation of the exchange energy at $\nu = 1$ in the $r_s \ll 1$ limit is about ~15% relative to the analytical values obtained in the HFA. Thus, one should treat the close match of ED data and experiment in Fig. 3(b) as a mutual compensation of two errors opposite in sign. At the same time, agreement within 20% seems to be quite legitimate. A dramatic reduction of the spin stiffness (or exchange energy) is evident from calculated data, whereas it is not obvious in terms of entangled electron states, redistributed over LLs (generally speaking, poorly defined).

The same situation can be considered in the formalism of a 2D Fermi liquid in *a weak magnetic field*. Fermi-liquid quasiparticles can have two opposite spin projections, and in the ground state only one of the Fermi spheres, with $S_z = -1/2(\downarrow)$, is filled [see the inset in Fig. 3(a)]. The states of the same type, differing only in the projection of the spin, should have the Zeeman splitting in energy. The simplest neutral excitation, which is SE, can be represented as a set of single-particle transitions from a filled Fermi sphere to an empty one but to states with some shift of the wave vector $\vec{k} \Rightarrow \vec{k} + \vec{q}$. The energy of such a one-particle transition is

$$E(\vec{k},\vec{q}) = E_\uparrow(\vec{k}+\vec{q}) - E_\downarrow(\vec{k}) = E_z + \frac{\hbar^2(\vec{k}+\vec{q})^2}{2m^*_{FL}} - \frac{\hbar^2\vec{k}^2}{2m^*_{FL}}.$$

Then the collective excitation energy will be a certain wave packet, constructed from such single-particle transitions in

accordance with some weight function $f(\vec{k})$:

$$E_{\mathrm{SE}}(q) = \langle 0| \sum_{\vec{k}} E(\vec{k},\vec{q})\, f(\vec{k})|0\rangle = \frac{\hbar^2 \vec{q}}{m^*_{FL}} \sum_{\vec{k}} \vec{k}\cdot f(\vec{k})$$

$$+\left[E_z + \frac{\hbar^2 q^2}{2m^*_{FL}}\right] \sum_{\vec{k}} f(\vec{k}),$$

where summation is carried out over the entire Fermi sphere. From the weight function $f(\vec{k})$, we need to know only its normalization condition and its even character $f(\vec{k}) = f(-\vec{k})$. Then we easily get

$$E_{\mathrm{SE}}(q) = E_z + \frac{\hbar^2 q^2}{2m^*_{FL}}. \tag{1}$$

This simple formula implies that for SEs in a Fermi liquid, the dispersion will be determined by the *renormalized mass of quasiparticles*. It is interesting that the dispersion relation, deduced in the theoretical study [14] using the diagrammatic technique, is reduced to a similar form:

$$E_{\mathrm{SE}}(q) = E_z + \frac{\hbar\omega_c}{2}(q l_B)^2 = E_z + \frac{\hbar^2 q^2}{2m^*_c}. \tag{2}$$

The principal difference is that in the latter formula, the mass is cyclotron. If that were the case, the collective excitation SEs would be insensitive to interaction, which is unlikely in a strongly interacting system. As is known from studies using the method of cyclotron resonance [15], the cyclotron mass in ZnO-based 2DESs is close in value to the conduction band parameter $m_c \approx 0.3m_0$. In contrast, the Fermi-liquid mass of quasiparticles is significantly enhanced for ZnO systems with high r_s values. This effective mass was probed using the magnetophotoluminescence method [6] and was extracted as a ratio of 2D electron density to the measured Fermi energy. The Fermi-liquid effective mass is enhanced approximately twofold in ZnO heterostructures with relevant electron densities. Therefore, in Fig. 3(b) the spin stiffness was also compared with expression (1) for the parameter $m^*_{FL} = 0.6m_0$ (dash-dotted line). This gives excellent agreement with the experimental data and thus supports the idea of the Fermi-liquid character of the SE dispersion.

IV. DISCUSSION

A similar answer about the rescaling of the exchange energy at $r_s \gg 1$ was obtained in [5] via the probing of the modified energy of the cyclotron spin-flip excitation at $\nu = 1$. However, the energy of that combined inter-LL excitation had several many-particle contributions, including exchange energies on initial and final LLs, the correlation energy. It was impossible to separate them experimentally or analytically, and therefore, the effect of softening the exchange contributions was described at the qualitative level, implying that they are all of the same order of magnitude.

Here we are dealing with the simplest type of spin excitations, the energy and dispersion of which include only the pure exchange energy of the quantum Hall ferromagnet. Thus, it became possible to quantitatively describe the spin stiffness of the system, as well as to find out its relationship with the Fermi-liquid parameters. Although it is experimentally impossible to probe the unperturbed spin gap of the SEs in the short-wavelength limit, it was verified using numerical calculations that the dispersion of the SEs is softened simultaneously in the long-wavelength and short-wavelength limits.

Both examples of the transformation of collective spin-flip excitations at $\nu = 1$ point to a unified evolution of the exchange energy contributions: the crossover between $E_C = e^2/\varepsilon l_B$ and $\hbar\omega_c$. This is in qualitative agreement with the analytical dependence, obtained within the framework of the excitonic representation [25], for the exchange energy needed for the formation of skyrmion-antiskyrmion pairs:

$$\Sigma = \frac{\sqrt{\pi/2}E_C\,\hbar\omega_c}{\sqrt{\pi/2}E_C + \hbar\omega_c} = \frac{\sqrt{4\pi}Ry^*}{r_s + \sqrt{\pi/4}\,r_s^2}. \tag{3}$$

The latter equality is rewritten in terms of the effective Rydberg energy and the dimensionless parameter $r_s = \sqrt{2}\,E_C/\hbar\omega_c$ for magnetic field corresponding to $\nu = 1$. The asymptote at $r_s \ll 1$ naturally coincides with the Hartree-Fock answer for the exchange energy on the lowest LL. In the limit of strong interaction, however, it reaches the value of the cyclotron energy. This extremely convenient formula was derived, nonetheless, on the assumption that the structure of the ground state remains unchanged—all electrons at $\nu = 1$ are on the lowest LL. Actually, the redistribution of electrons over a few LLs causes a significant polarizability of the incompressible 2DES. This in turn weakens the interaction between electrons and leads to the further reduction of the many-particle energy terms. Qualitatively, this modification of interaction can be considered within the static screening approximation [20,21]. The functional dependence of many-particle energies on r_s at $\nu = 1$ then turns out to be similar to formula (3).

The ongoing modification of the quantum Hall state $\nu = 1$ is interesting not only in terms of changing the energy scales but also from the point of view of transforming its internal structure. This can be seen by inspecting the pair correlation function. The latter is calculated by exact diagonalization of the ground state with $N_E = 10$ and explicit accounting of six LLs. Figure 4 shows an example of the obtained distribution for the sample $n_s = 2.85 \times 10^{11}$ cm^{-2} in comparison with the well-known exact answer for the limit $r_s \ll 1$. A number of additional features can be seen in the behavior of $g(r)$. For a strongly interacting system it reveals a correlation hole up to distances $r \sim 1.5l_B$, two times lower steepness at $r \lesssim l_B$, and a petal at $r \sim 2.5l_B$. Thus, the spread of electrons over several different LLs inevitably suppresses the value of the exchange integral—electrons just have different quantum numbers. Meanwhile, the Coulomb correlations are strongly modified relative to the classical case with weak interaction. The appearance of additional petals in the function $g(r)$ can be regarded as a prerequisite for the transition from a liquid to a strongly correlated Wigner crystal. Lowering the filling factor to values $\nu < 1$ will further suppress exchange interaction and increase the role of correlations.

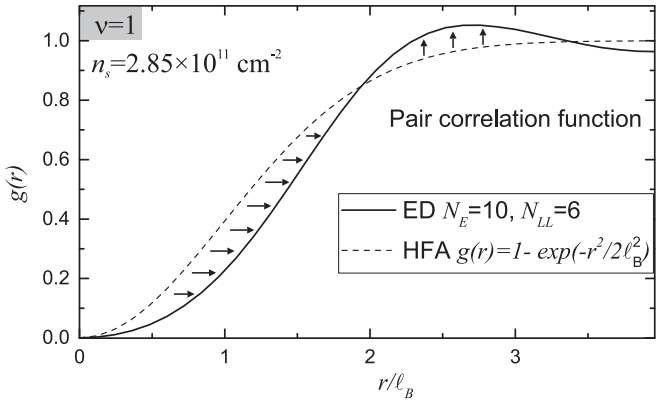

FIG. 4. The pair correlation function of 2DES at $\nu = 1$, calculated by exact diagonalization (solid curve) and HFA result (dashed curve). The calculation parameters and the electron density are given therein.

V. CONCLUSION

In conclusion, we observed anomalous behavior of spin stiffness in the quantum Hall ferromagnet at $\nu = 1$ with strong Coulomb interaction and the Wigner-Seitz parameter $r_s > 6$. To achieve that, Raman scattering experiments were performed on MgZnO/ZnO high-quality heterostructures, containing 2DESs with different densities. The k dispersions of spin excitons were explicitly measured. The spin stiffness grows linearly with electron density and is reduced many-fold with respect to the energy scale $e^2/\varepsilon\text{ł}_B$ to values of the cyclotron energy for the Fermi-liquid quasiparticles. This answer was not known before, and in a certain sense it is reassuring since the collective effects in a strongly interacting electron system could hardly depend only on single-particle band parameters. The Fermi-liquid effective mass is more in the spirit of Landau's theory. The simulations by exact diagonalization agree well with the experimental data and also confirm the Fermi-liquid values for spin stiffness.

ACKNOWLEDGMENTS

The authors are grateful to the Russian Science Foundation (Grant No. 19-42-04119) for their support in performing experiments on Raman scattering and RFBR (Grant No. 20-02-00343) for support in performing the calculations. We thank S. M. Dickmann for fruitful discussions.

[1] J. Falson, Y. Kozuka, J. H. Smet, T. Arima, A. Tsukazaki, and M. Kawasaki, Appl. Phys. Lett. **107**, 082102 (2015).
[2] J. Falson *et al.*, Nat. Phys. **11**, 347 (2015).
[3] A. B. Van'kov, B. D. Kaysin, and I. V. Kukushkin, Phys. Rev. B **96**, 235401 (2017).
[4] D. Maryenko, J. Falson, Y. Kozuka, A. Tsukazaki, and M. Kawasaki, Phys. Rev. B **90**, 245303 (2014).
[5] A. B. Van'kov, B. D. Kaysin, S. Volosheniuk, and I. V. Kukushkin, Phys. Rev. B **100**, 041407(R) (2019).
[6] V. V. Solovyev and I. V. Kukushkin, Phys. Rev. B **96**, 115131 (2017).
[7] I. V. Kukushkin and S. Schmult, Phys. Rev. B **101**, 235152 (2020).
[8] C. Kallin and B. I. Halperin, Phys. Rev. B **30**, 5655 (1984).
[9] M. Dobers, K. von Klitzing, and G. Weimann, Phys. Rev. B **38**, 5453 (1988).
[10] S. L. Sondhi, A. Karlhede, S. A. Kivelson, and E. H. Rezayi, Phys. Rev. B **47**, 16419 (1993).
[11] S. E. Barrett, G. Dabbagh, L. N. Pfeiffer, K. W. West, and R. Tycko, Phys. Rev. Lett. **74**, 5112 (1995).
[12] Yu. A. Bychkov, S. V. Iordanskii, and G. M. Eliashberg, JETP Lett. **33**, 143 (1981).
[13] I. K. Drozdov, L. V. Kulik, A. S. Zhuravlev, V. E. Kirpichev, I. V. Kukushkin, S. Schmult, and W. Dietsche, Phys. Rev. Lett. **104**, 136804 (2010).
[14] S. V. Iordanski and A. Kashuba, J. Supercond. **16**, 783 (2003).
[15] V. E. Kozlov, A. B. Van'kov, S. I. Gubarev, I. V. Kukushkin, V. V. Solovyev, J. Falson, D. Maryenko, Y. Kozuka, A. Tsukazaki, M. Kawasaki, and J. H. Smet, Phys. Rev. B **91**, 085304 (2015).
[16] A. V. Schepetilnikov and Yu. A. Nefedov (unpublished).
[17] A. B. Van'kov, B. D. Kaysin, V. E. Kirpichev, V. V. Solovyev, and I. V. Kukushkin, Phys. Rev. B **94**, 155204 (2016).
[18] F. D. M. Haldane, Phys. Rev. Lett. **55**, 2095 (1985).
[19] A. B. Van'kov and I. V. Kukushkin (unpublished).
[20] A. P. Smith, A. H. MacDonald, and G. Gumbs, Phys. Rev. B **45**, 8829 (1992).
[21] I. L. Aleiner and L. I. Glazman, Phys. Rev. B **52**, 11296 (1995).
[22] W. Luo and R. Cote, Phys. Rev. B **88**, 115417 (2013).
[23] A. B. Vankov, B. D. Kaysin, and I. V. Kukushkin, Phys. Rev. B **98**, 121412(R) (2018).
[24] W. Luo and T. Chakraborty, Phys. Rev. B **93**, 161103(R) (2016).
[25] S. Dickmann, Phys. Rev. B **65**, 195310 (2002).